JOURNAL OF MATERIALS SCIENCE: MATERIALS IN MEDICINE 13 (2002) 1221–1225

Influence of the non-bridging oxygen groups on the bioactivity of silicate glasses

J. SERRA*, P. GONZÁLEZ, S. LISTE, S. CHIUSSI, B. LEÓN, M. PÉREZ-AMOR
Department of Applied Physics, University of Vigo, Lagoas-Marcosende 9, 36200 Vigo, Spain
H. O. YLÄNEN, M. HUPA
Process Chemistry Group, Combustion and Materials Chemistry, Åbo Akademi University, Turku, Finland

The effect of the composition and bonding configuration of the bioactive silica-based glasses on the initial stage *in vitro* bioactivity is presented.
Information of the IR active Si–O groups of glass in the system SiO_2–P_2O_5–CaO–Na_2O–K_2O–MgO–B_2O_3 was obtained by fourier transform Infrared (FTIR) spectroscopy. Two different bands associated to non-bridging oxygen stretching vibrations (Si–O–1NBO and Si–O–2NBO) and a gradual shifting of the bridging oxygen stretching vibration (Si–O) have been observed and evaluated. Both effects are attributed to a decrease of the local symmetry originating from the incorporation of alkali ions into the vitreous silica network. The Si–O–NBO(s)/Si–O(s) absorbance intensity ratio increases with a gradual incorporation of the alkali ions (diminution of SiO_2 content) following a linear dependence up to values close to 50 wt % of SiO_2.
In vitro test analysis by scanning electron microscopy (SEM) and energy dispersive X-ray analysis (EDXA) showed a correlation between the amount and type of the non-bridging oxygen functional groups and the growth of the silica-rich and CaP layers. It was found that a minimum concentration of Si–O–NBO bonds in the glass network is required in order to have an efficient ion exchange and dissolution of the silica network. Finally, the bioactivity of the glass is favored by the presence of the Si–O–2NBO groups in the glassy network. The role of these functional groups in the dissolution of the silica network through the formation of silanol groups and the adsorption of water is discussed.

Introduction

Bioactive glasses are of great interest for the medical applications due to their osteoconductive and osteoinductive properties [1, 2]. One of the main characteristics of the bioactive glasses [1–3] are their highly reactive surface when this material is soaked in human plasma or an analogous solution. It is known that a partial dissolution of the bioactive glass surface occurs leading to the formation of a silica-rich gel layer and, subsequently the precipitation of a calcium phosphate layer on the bioactive material takes place [1, 2, 5, 6].

The bioactive silica-based materials have an open network structure consisting of SiO_x tetrahedrons. The open structure enables the accommodation of alkali and alkali-earth cations. These cations act as network modifiers (Na^+, K^+, Ca^{2+}) and provoke the disruption of the continuity of the glassy network due to the breaking of some of the Si–O–Si bonds thus leading to the formation of non-bridging oxygen groups (Si–O–NBO)[4].

Several spectroscopic techniques are sensitive to changes in the composition and the bonding configuration of the glasses [3, 7]. Fourier transform infrared (FTIR) spectroscopy provides valuable information on the local structure of silicate glasses [8–12] which allows us to determine changes on the Si–O–Si vibrational modes and the identification of the Si–O–NBO functional groups. Surprisingly, despite silica-based glasses being extensively studied, and the presence of the Si–O–NBO groups as a function of the glass silica content is a well established fact, until now the infrared spectroscopy has not been widely applied to the study of this special subgroups of glasses.

Thus, the aim of this work is to evaluate, by FTIR spectroscopy, the concentration of the non-bridging oxygen groups in the bioactive glasses and to clarify its role in the initial stages of the *in vitro* bioactivity of the glass.

* Author to whom all correspondence should be addressed.

TABLE I Composition of the glasses

Wt%	Na_2O	K_2O	CaO	P_2O_5	MgO	B_2O_3	SiO_2
Glass #1	5	5	17	2	5	—	66
Glass #2	10	5	15	3	5	3	59
Glass #3	21	9	8	4	2	1	55
Glass #4	15	15	15	—	2	3	50
Glass #5	20	10	20	3	5	—	42

Materials and methods

In the current work bioactive glasses with different compositions (Table I) in the system SiO_2–P_2O_5– CaO–Na_2O–K_2O–MgO–B_2O_3 have been studied. The experimented bioactive glasses were made by mixing analytical grade $Na_2CO_3, K_2CO_3, CaCO_3$, $CaHPO_4, CaHPO_4 \cdot 2H_2O$, MgO, H_3BO_3 and commercial Belgian quartz sand. The batches were melted in a Pt-crucible at 1360 °C for 3 h. The glasses were cast, annealed, crushed, and remelted to improve homogeneity. In the final casting, a graphite mold with a round hole (20 mm diameter and 100 mm deep) was used. The test pieces were obtained by sawing from the round bioactive glass bars discs of 2 mm thick. The discs were washed and stored in ethanol.

Information on the IR active Si–O groups present in the glasses was obtained by FTIR spectroscopy with a Bruker IFS 28 Fourier transform infrared spectrometer in the mid-IR range from 550 to 5000 cm^{-1} with a resolution of 0.2 cm^{-1}.

The *in vitro* tests [13] were carried out by immersing the experimented glasses in simulated body fluid (SBF) for 72 h at 37.0 $\pm$ 0.5 °C in polystyrene containers. In the study, the approximate glass surface area (SA) to SBF volume (V) ratio, SA/V was 0.5 cm^{-1}. Four different glasses (glass # 2, 3, 4, and 5) were studied and, for the statistics, five identical pieces of each composition were analyzed. After immersion in the SBF, the surface layers of the glasses were analyzed by back-scattered electron imaging of a scanning electron microscope equipped with energy dispersive X-ray analysis (BEI-SEM/EDXA, LEO s 360, formerly Cambridge Instruments Ltd., UK). For the analyses, the glass discs were embedded in isobornylmethacrylate. After hardening of the acrylate the specimens were ground in the cross-sectional plane perpendicular to the long axes of the disc until the section area in the middle of each disc was reached. The polished surface of each specimen was carbon coated (Temcarb TB500 sputter coater, Emscope Laboratories Ltd., Ashford, UK).

Results

In Fig. 1 the infrared absorption spectra of the experimented bioactive glasses with different composition (Table I) are shown. The absorbance of the spectra were compared to values given in the literature [9, 12, 14]. In spectrum (i) the IR bands are identified as follows: the Si–O(s) stretching mode is located in the range 1000–1200 cm^{-1}, the Si–O(b) bending mode is found around 800 cm^{-1}, and the band between 890 and 975 cm^{-1} is associated to the Si–O(s) with one non-bridging oxygen (Si–O–NBO) per SiO_4 tetrahedron (Q^3 groups). As well, it can be observed (Fig. 1, (ii)–(iv)) that, when the SiO_2 concentration decreases (increasing of the alkali and alkali-earth oxide content), the position of the maximum absorbance of the Si–O (s) band shifts towards lower values, until 1034 cm^{-1}. The intensity of the band decreases simultaneously. Additionally, the Si–O bending vibration decreases and the intensity of the band associated to the Si–O–NBO groups increases and becomes sharper. In spectrum (iv), the emerging of a new

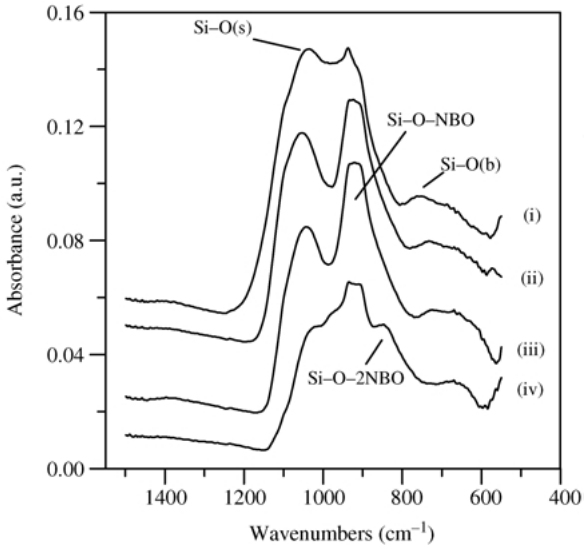

Figure 1 Infrared absorbance spectra of bioactive glasses with: (i) 59, (ii) 55, (iii) 50, and (iv) 42 wt % SiO_2.

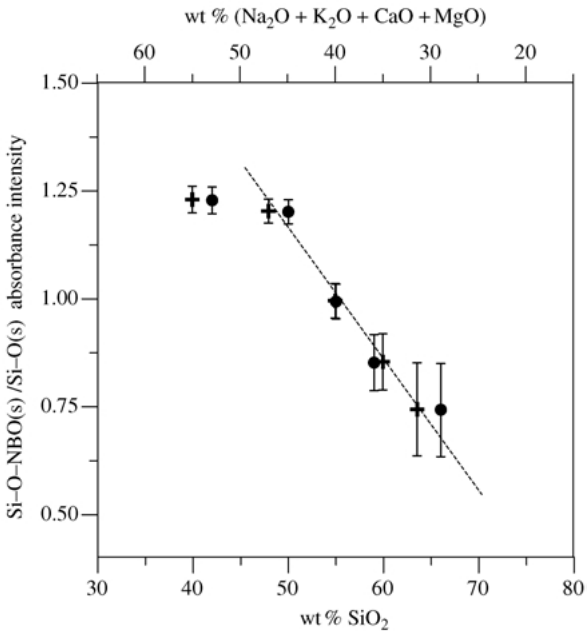

Figure 2 Si–O–NBO (s)/Si–O (s) absorbance intensity ratio as a function of glass composition: (•) SiO_2 and (+) alkali and alkali-earth oxide content.

band centered at 840 cm^{-1} is clearly observed, which is assigned to the Si–O(s) with two non-bridging oxygen per SiO_4 tetrahedron (Si–O–2NBO), also called Q^2 groups [12]. For glasses with high alkali and alkali-earth oxide content (55%), the Q^3 groups are progressively converted to Q^2 groups, according to the gradual incorporation of the ions in the glass structure.

The presence of IR bands associated to Si–O–NBO and Si–O–2NBO groups indicate that the vitreous silica network suffers a net decrease in its local symmetry by the addition of alkali ions. In other glass types with a certain percentage of alkali oxides a similar behavior has also been observed [3, 12].

As described by the central force model [15] the shifting of the Si–O(s) vibration frequency is due to structural changes associated to variations of the intertetrahedral Si–O–Si bond angle (θ). Therefore, for pure fused silica glasses in an unstressed configuration the Si–O(s) band would be located at 1080 cm^{-1}, which corresponds to an intertetrahedral angle of 150°. When alkali ions are introduced in the vitreous silica network, a structural rearrangement in the Si–O–Si environment takes place leading to lower intertetrahedral angle values and a strained network. This results in important Si–O(s) vibrational changes due to a decrease of the local symmetry.

To clarify the relative contribution of each IR-active Si–O group, the absorbance intensities of the Si–O–NBO and the Si–O stretching modes have been studied. Fig. 2 shows the Si–O–NBO(s)/Si–O(s) intensity ratio as a function of the glass composition. With the gradual incorporation of the alkali ions (diminution of SiO_2 content) up to values close to 50 wt % a linear dependence was found. For higher alkali and alkali-earth oxide concentrations it can be observed that this relationship tends to the saturation, indicating that the Si–O–NBO groups decrease due to the transformation of the Q^3 in Q^2 groups (Fig. 1 (iv)).

In order to analyze the role of the non-bridging oxygen groups on bioactivity of the glass, *in vitro* tests by soaking the glasses in simulated body fluid were carried out. As expected, the glass with a silica content exceeding 60% (Glass #1) does not give a bioactive response. Fig. 3 shows the SEM-EDX analysis of the Glass #2 (59 wt % SiO_2) on which a surface scrap with a high Si and O content can be observed. Dissolution of the glass surface and, consequently, a release of alkali ions occurs to a certain extent but the formation of a CaP layer is not detected. For glasses with a silica content ranging from 55% to 42% (Glasses #3, 4, and 5) the typical bioactive behavior was observed. Fig. 4 shows the cross section analysis by BEI-SEM and EDX. In the cross section three different zones were identified: from right to left, the original glass; an intermediate silica-rich layer and the formation of a calcium and phosphorous rich layer. The chemical composition and the thickness of the two surface layers were evaluated for each glass (Fig. 5). According to these measurements, the thickness of both layers decreases when the SiO_2 content of the glass increases (decreasing of the alkali and alkali-earth oxide content). Moreover, for all the glasses with a silica-rich layer it was six–seven times thicker than that of the CaP layer. This indicates that the growth of the CaP film depends on the leaching depth of alkali ions and, consequently, on the thickness of the silica film formed.

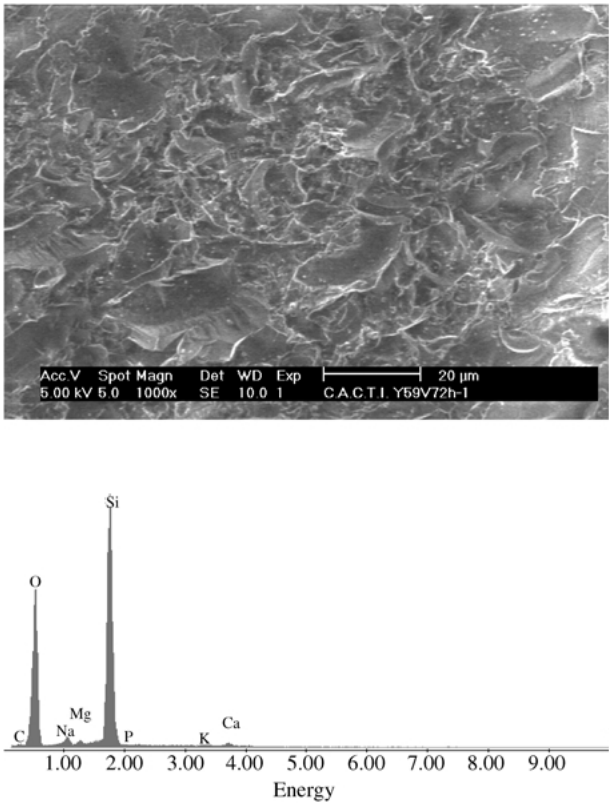

Figure 3 BEI-SEM micrograph and EDX analysis of Glass #2 (59 wt % SiO_2) after 72 h of immersion in simulated body fluid.

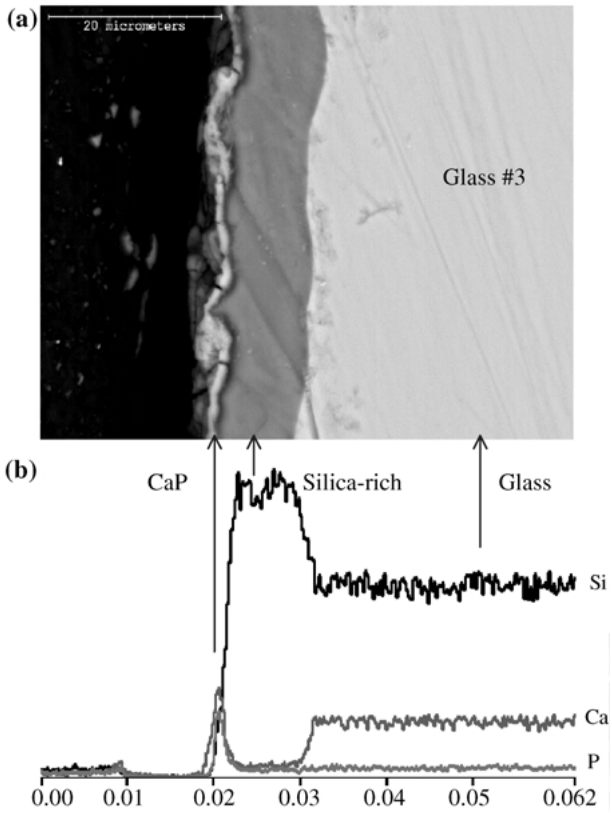

Figure 4 (**a**) BEI-SEM micrograph and (**b**) EDXA line-profiles of Si, Ca and P scanned over a cross section of bioactive Glass #3 after 72 h of immersion in SBF. The line-profiles shown the bulk glass, the silica-rich layer and the calcium phosphate film.

Discussion

According to Hench *et al*. [1, 2], the reactions of the bioactive glasses can be divided into five stages: (i) rapid exchange of alkali or alkali-earth elements with H^+ or H_3O^+ from the surrounding solution, (ii) loss of soluble silica in the form of $Si(OH)_4$ to the solution resulting from the breakage of Si–O–Si bonds and formation of Si–OH (silanols) at the glass solution interface, (iii) condensation and repolymerization of the SiO_2-rich surface layer, (iv) migration of Ca^{2+} and PO_4^{3-} groups through the SiO_2-rich layer and the formation of a CaO–P_2O_5-rich film on top of the SiO_2-rich layer, and (v) crystallization of the CaO–P_2O_5-rich film and formation of an apatite layer.

The results presented here contribute to improving the understanding of the initial stages (i and ii) of the surface reaction on a bioactive glass.

First, the ion exchange (stage i) is favored by the presence of Si–O–NBO groups in the glass network and a minimum concentration of this group is required in order to have an efficient ion exchange. The incorporation of alkali and alkali-earth elements in the silica matrix leads to a disruption of the network and promotes the formation of non-bridging oxygen groups. These elements are commonly known as network modifiers but are not a part of the glass network, and thus facilitates the ion exchange. An increase of the alkali and alkali-earth content creates a larger number of non-bridging oxygen groups in the glass structure leading to a higher dissolution rate of the silica. The IR spectroscopy provides useful information (Fig. 1) needed to quantify the concentration of Si–O–NBO groups in the bioactive glasses. Assuming that both Si–O–NBO and Si–O groups have same bond strength [16], from the intensity of the IR absorption bands (Figs. 1 and 2) the concentration of bonds can be calculated by the equation $N = K \int \alpha(\omega)\, d\omega$, where N is the number of bonds per cm^3, $\alpha(\omega)$ is the absorption coefficient at wave number ω and K is a constant value [17]. By comparison of the values depicted in Fig. 2 and the bioactive response shown in Fig. 5 it can be concluded that a ratio ≥ 1 between the Si–O–NBO and the Si–O groups is required in order to have an efficient ion exchange, dissolution of the silica and formation of a SiO_2-rich layer on the surface. Figs. 3 and 5 demonstrate that, in this range of glass compositions, for Si–O–NBO/Si–O ratios lower than 1 the rate of silica dissolution is greatly reduced and, therefore, the migration of Ca^{2+} and PO_4^{3-} groups to the surface in order to form a CaP rich layer is prevented.

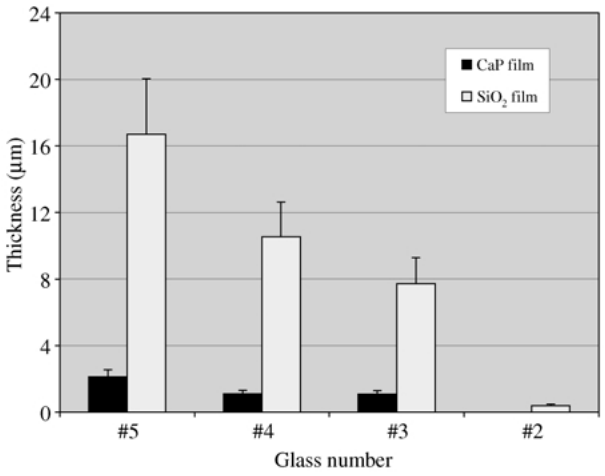

Figure 5 Thicknesses of the CaP and silica-rich layers of the each bioactive glass shown in Table I.

Second, our results also contribute to clarify the role of the silanols in the dissolution rate of the silica (stage ii). Fig. 1 shows that the IR spectroscopy is sensitive to differentiate the presence of 1NBO and 2NBO groups in the glasses. The results shown in Fig. 5 indicate that the presence of 2NBO groups in the glass favors the bioactive process. It can be observed that for the glasses with a silica content of 42%, which exhibit the presence of 2NBOs (Fig. 1 (iv)), the thickness of the silica-rich and CaP layers is nearly double that of the other two glasses (Fig. 5). This indicates that the content of the Si–O–2NBO groups in the glass network plays a key role in the dissolution rate of the silica through the formation of Si–OH groups at the glass surface. The contribution of the silanol groups can be explained according to the work of Helms and Poindexter [18] on the microstructure and imperfections of the silicon-dioxide. Most of the water in the amorphous SiO_2 network is normally bonded as silanol or OH groups to Si atoms which are not fourfold coordinated to oxygen. These functional groups can be

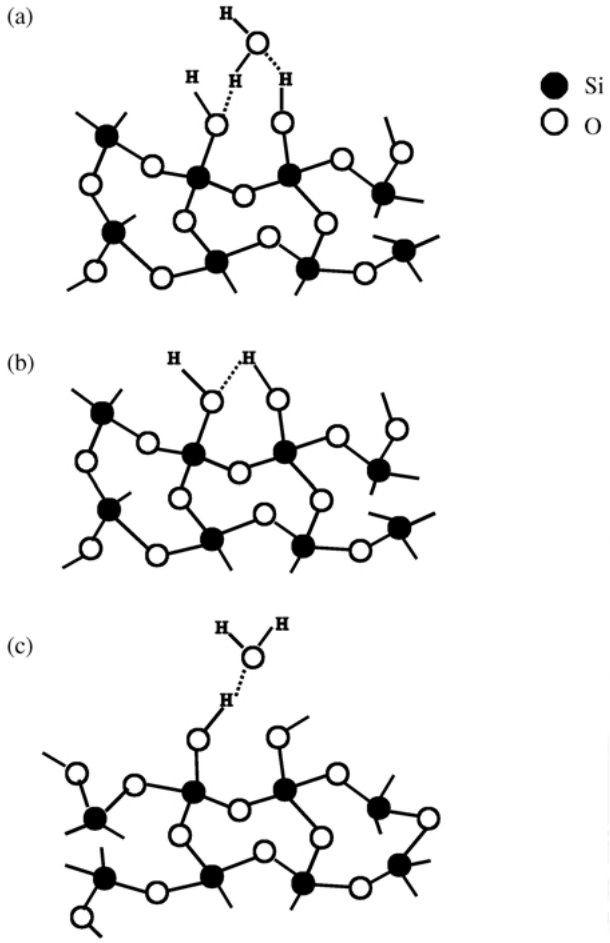

Figure 6 Disposition of hydrogenous species in amorphous silica proposed by Helms and Poindexter [18]: (a) H_2O physisorbed onto two adjacent or vicinal silanols; (b) vicinal silanols in normal H-bonded configuration, representing chemisorbed H_2O; (c) H_2O physisorbed onto isolated silanol.

present in an a-SiO_2 network as isolated silanol groups (i.e. originated by 1NBO) or adjacent Si–OH groups to one or more other silanols (i.e. originated by 2NBO groups). A pair of silanols immediately adjacent and bonded by H bridge (Fig. 6) would lead to the incorporation of a chemisorbed H_2O molecule in silica, and as well physisorbed water can be obtained on two adjacent silanols or onto isolated silanol. Finally, non-adsorbed H_2O would be viable entities in SiO_2, perhaps in a variable equilibrium with the physi- or chemisorbed H_2O. Thus, the presence of the Si–O–2NBO groups facilitates the incorporation of adsorbed water and subsequently the dissolution of the silica network. For an increasing silica solubility rate, higher migration of Ca^{2+} and PO_4^{3-} groups to the surface takes place which favors the formation of the CaP-rich layer.

Conclusions

A study of the effect of the glass bonding configuration on the initial stages of the *in vitro* bioactive process in the system SiO_2–P_2O_5–CaO–Na_2O–K_2O–MgO–B_2O_3 have been carried out.

Using FTIR analysis two different bands associated with the non-bridging oxygen stretching vibration (Si–O–NBO) have been identified and a gradual shifting of the bridging oxygen stretching vibration (Si–O) have been observed and evaluated.

In vitro test analysis has demonstrated a correlation between the amount and type of the non-bridging oxygen functional groups and the growth of the silica-rich and CaP layers. It is demonstrated that the ion exchange is favored by the presence of Si–O–NBO bonds in the glass network and a minimum concentration is required in order to have an efficient ion exchange, dissolution of the silica and formation of a SiO_2-rich layer on the surface. It is also demonstrated that the content of the Si–O–2NBO groups in the glass network favors the bioactive process and plays a key role in the dissolution rate of the silica through the formation of adjacent silanol (Si–OH) groups at the glass surface and the incorporation of adsorbed water.

Acknowledgments

The authors wish to thank Dr A. Zocco and A. Fernández for their collaboration during the experimental work, and J. B. Rodríguez (CACTI) for SEM and EDS analyzes. This work was supported by Xunta de Galicia (PGIDT99PXI32101B), Universidad de Vigo (64502I908 and 6452I106) and Ministerio de Ciencia y Tecnología (MAT2001-3434). The authors wish also to thank Ms D. Zhang at Åbo Akademi University for manufacturing the bioactive glass discs.

References

1. L. L. HENCH and J. WILSON (eds.) ''An Introduction to Bioceramics'' (World Scientific, Singapore, 1993).
2. T. YAMAMURO, L. L. HENCH and J. WILSON (eds.) ''Handbook of Bioactive Ceramics'' (CRC Press, Boca Raton FL, 1990).
3. P.GONZÁLEZ, J. SERRA, S. LISTE, S. CHIUSSI, B. LEÓN and M. PÉREZ-AMOR, *Vacuum* **67** (2002) 647.
4. H. SCHOLZE ''Glass: Nature, Structure and Properties'' (Springer-Verlag, New York, 1990).
5. K. H. KARLSSON and H. O. YLÄNEN, in ''Proceedings Book of Advances in Science and Technology 28 and 9th Cimtec-World Forum on New Materials, Florencia, June 1998'', edited by P. Vincenzini (Techna, Italy, 1999).
6. Z. STRAND, *Biomaterials* **13** (1978) 862.
7. R. W. CAHN, P. HAASEN and E. J. KRAMER (eds.) ''Materials Science and Technology; Glasses and Amorphous Materials'' (VCH Publishers, New York, 1991).
8. W. A. PLISKIN, *J. Vac. Sci. Technol.* **14** (1977) 1064.
9. P. LANGE, *J. Appl. Phys.* **66** (1989) 201.
10. P. LANGE, U. SCHNAKENBERG, S. ULLERICH and J. SCHLIWINSKI, *ibid.* **68** (1990) 3532.
11. F. L. GALEENER and G. LUCOVSKY, *Physical Review Letters* **37** (1976) 1474.
12. D. M. SANDERS, W. B. PERSON and L. L. HENCH, *Applied Spectroscopy* **28** (1974) 247.
13. T. KOKUBO, M. TANAHASHI, T. YAO, M. MINODA, T. MIYAMOTO, T. NAKAMURA and T. YAMAMURO, *Bioceramics* **6** (1993) 327.
14. P. G. PAI, S. S. CHAO, Y. TAKAGI and G. LUCOVSKY, *J. Vac. Sci. Technol. A* **4** (1986) 689.
15. E. G. PARADA, P. GONZÁLEZ, J. POU, J. SERRA, D. FERNÁNDEZ, B. LEÓN and M. PÉREZ-AMOR, *ibid.* **14** (1996) 436.
16. K. AWAZU, *J. Non-Cryst. Solids* **260** (1999) 242.
17. A. C. ADAMS, *Solid State Technol.* **26** (1983) 135.
18. C. R. HELMS and E. A. POINDEXTER, *Rep. Prog. Phys.* **57** (1994) 791.

Received 24 May
and accepted 29 May 2002